International Journal of Geosciences, 2024, 15, 70-86
https://www.scirp.org/journal/ijg
ISSN Online: 2156-8367
ISSN Print: 2156-8359

Antecedent Precipitation Index to Estimate Soil Moisture and Correlate as a Triggering Process in the Occurrence of Landslides

Marcio Augusto Ernesto De Moraes[1], Walter Manoel Mendes Filho[2], Rodolfo Moreda Mendes[1], Cassiano Antonio Bortolozo[1], Daniel Metodiev[1], Marcio Roberto Magalhães De Andrade[1], Harideva Marturano Egas[1], Tatiana Sussel Gonçalves Mendes[3], Luana Albertani Pampuch[3]

[1]CEMADEN - National Centre for Monitoring and Early Warnings of Natural Disasters, General Coordination of Research and Development, São José dos Campos, Brazil
[2]Faculty of Science and Technology, Goias Federal University, Aparecida de Goiânia, Brazil
[3]Institute of Science and Technology, São Paulo State University (Unesp), São José dos Campos, Brazil
Email: marcio.moraes@cemaden.gov.br

How to cite this paper: De Moraes, M.A.E., Filho, W.M.M., Mendes, R.M., Bortolozo, C.A., Metodiev, D., De Andrade, M.R.M., Egas, H.M., Mendes, T.S.G. and Pampuch, L.A. (2024) Antecedent Precipitation Index to Estimate Soil Moisture and Correlate as a Triggering Process in the Occurrence of Landslides. *International Journal of Geosciences*, **15**, 70-86.
https://doi.org/10.4236/ijg.2024.151006

Received: December 11, 2023
Accepted: January 28, 2024
Published: January 31, 2024

Abstract

Landslides are highly dangerous phenomena that occur in different parts of the world and pose significant threats to human populations. Intense rainfall events are the main triggering process for landslides in urbanized slope regions, especially those considered high-risk areas. Various other factors contribute to the process; thus, it is essential to analyze the causes of such incidents in all possible ways. Soil moisture plays a critical role in the Earth's surface-atmosphere interaction systems; hence, measurements and their estimations are crucial for understanding all processes involved in the water balance, especially those related to landslides. Soil moisture can be estimated from *in-situ* measurements using different sensors and techniques, satellite remote sensing, hydrological modeling, and indicators to index moisture conditions. Antecedent soil moisture can significantly impact runoff for the same rainfall event in a watershed. The Antecedent Precipitation Index (API) or "retained rainfall," along with the antecedent moisture condition from the Natural Resources Conservation Service, is generally applied to estimate runoff in watersheds where data is limited or unavailable. This work aims to explore API in estimating soil moisture and establish thresholds based on landslide occurrences. The estimated soil moisture will be compared and calibrated using measurements obtained through multisensor capacitance probes installed in a high-risk area located in the mountainous region of Campos do Jordão municipality, São Paulo, Brazil. The API used in the calculation has been modified, where the recession coefficient depends on air temperature variability as well as the climatological mean temperature, which can be considered as losses in the water balance due to evapotranspiration. Once the API is calibrated, it will be used to extrapolate to the entire watershed and consequently estimate soil moisture. By utilizing recorded mass movements and comparing them with API and soil moisture, it will be possible to determine thresholds, thus enabling anticipation of landslide occurrences.

Keywords

Landslides, Antecedent Precipitation Index, Soil Moisture, Threshold, Water Balance

1. Introduction

Mass movements, particularly soil landslides, are considered frequent natural disasters that result in loss of human lives and substantial economic losses [1]. In Brazil, the most affected regions are the densely urbanized slopes, primarily located in the major urban centers of the South, Southeast, and Northeast. In the South and Southeast regions, the mass movement majority occurrences happen in the occupied slopes of the mountainous coastal areas of Brazil [2] [3]. In the Northeast region, according to the Brazilian Atlas of Natural Disasters (2013), the occurrences are concentrated in Bahia and Pernambuco, which have characteristics of barrier formation [4].

The primary preparatory and triggering environmental variable for landslide processes is rainfall. Once in Brazil there are several climate conditions [5], certain rainfall indices, such as accumulated rainfall over 24 hours, 48 hours, or 72 hours obtained through empirical correlation methods [6] [7] [8] are typically employed in Preventive Civil Defense Plans as critical operational thresholds in alert systems to predict landslides in urbanized slopes. However, relying solely on rainfall thresholds does not allow for precise and consistent issuance of alerts, as the landslide initiation process involves other equally important geo-environmental factors or variables.

In this context, geo-environmental or geotechnical variables, namely matric suction, and soil moisture [9] [10] are prominent. Understanding the behavior of these variables in unsaturated soils is crucial for better comprehension of the landslide rupture mechanism on urban slopes and consequently defining more precise and robust critical operational thresholds [11] [12]. These thresholds can be used in conjunction with rainfall thresholds (accumulated and intensity) to predict the occurrence of this type of process.

Soil moisture is a geotechnical variable that can be obtained through direct *in-situ* measurements using real-time monitoring sensors/equipment [13] or estimated through various empirical techniques or methods [14]-[22]. This estimation may also involve utilizing monitoring data for calibration or adjustment of prediction models [23]-[28].

Soil moisture estimates based on models can cover a wide range of spatial and temporal scales, as well as their complexity. A widely used approach to infer soil moisture is based on the Antecedent Precipitation Index (API), which is calculated by summing up the antecedent daily rainfall, weighted by a specific factor to be determined. This factor may encompass the entire complexity of soil characteristics and processes due to a rainfall event.

Therefore, this study aims to estimate soil moisture and establish critical operational thresholds based on past landslide occurrences, using an empirical modeling of the Antecedent Precipitation Index (API). This will be achieved by utilizing field measurements of soil moisture obtained through sensors and equipment utilizing multisensor capacitance, installed in a high-risk area located in the mountainous region of Campos do Jordão municipality, São Paulo, Brazil.

2. Study Area and Data Source

The municipality of Campos do Jordão is situated in the state of São Paulo, bordering Minas Gerais, precisely in the mountainous region known as Serra da Mantiqueira, which is part of the Atlantic Plateau. The area features altitudes ranging from 922 meters in the Rio Sapucaí valley near the border with the Municipality of Piranguçu (Minas Gerais) to 2008 meters in the region of Fazenda da Lavrinha in Guaratinguetá (SP). **Figure 1** illustrates the location of Campos do Jordão, the digital elevation model of the terrain, and the specific area referred to as the "monitoring region" in this study.

The urban region of Campos do Jordão is situated in the plateau compartment known as Planalto de Campos do Jordão, characterized by hilly terrain with restricted ridges. The area features rounded hilltops, slopes with rectilinear and sometimes steep profiles, high-density drainage, dendritic to pinnate patterns, closed valleys with restricted interior plains [29].

The terrain is supported by metamorphic rocks with granitic intrusions, following a regional NE direction structuring by metamorphic foliation and shear zones in the Precambrian rocks. Notably, the Jundiuvira Fault is located at the edge of the Campos do Jordão Plateau, adjacent to the escarpment of Serra da Mantiqueira. The predominant rocks consist of gneisses and migmatites from the Paraíba do Sul Complex [30]. Unconsolidated materials are found in the form of sedimentary deposits and residual soils.

Significant packages of organic clay occur in amphitheater erosive floodplains. Residual soils overlaid on crystalline rock slopes correspond to cambisols [31]. The textural variation of these soils results from the heterogeneity of the gneiss-migmatite rock mass, generally composed mainly of silt and fine sand, with variable occurrences of clay depending on the degree of profile alteration. The saprolitic material formed beneath the residual horizons, resulting from the decomposition of the gneiss-migmatite rock, exhibits a predominantly sandy-clayey texture, with the quantity of silt and clay varying with depth.

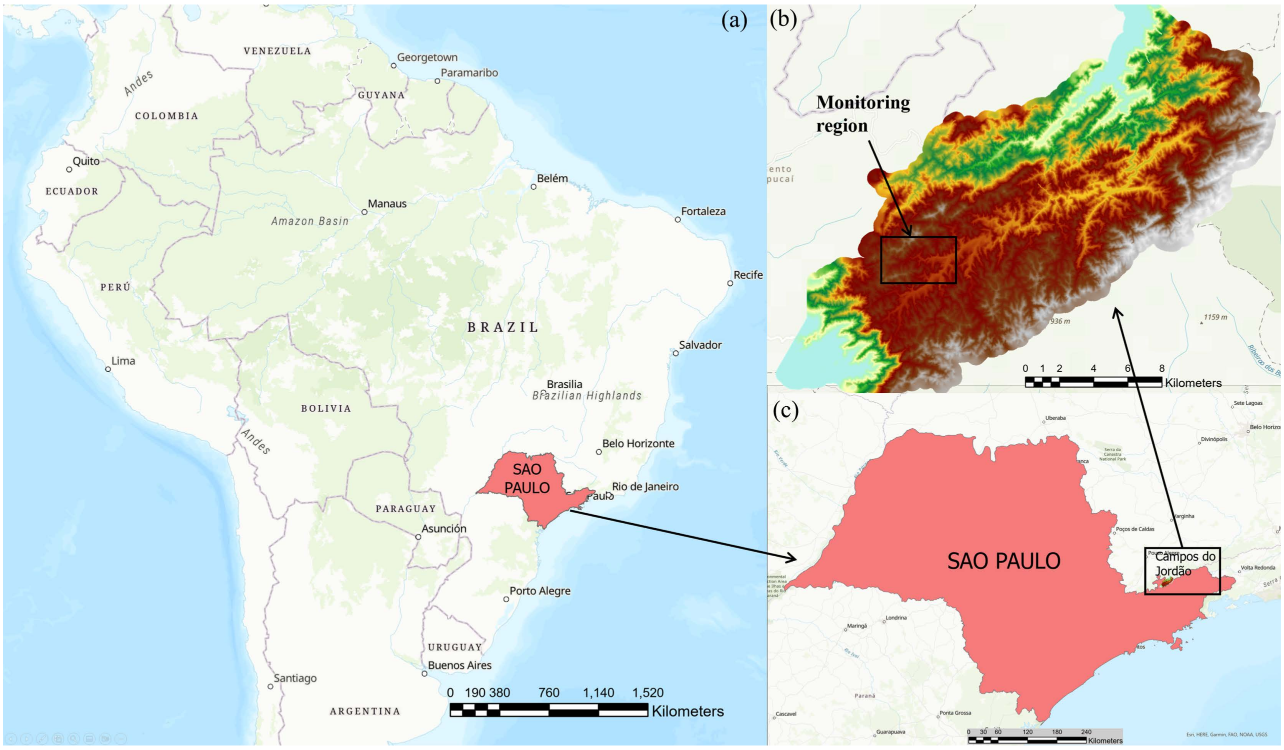

Figure 1. Noise-free Modelling. In (a) the forward calculation for the VES case, in (b) forward calculation for TEM sounding and in (c) the results for the simultaneous modelling of both methodologies.

The annual mean temperatures vary around 14˚C, with minimums below 0˚C and maximums potentially exceeding 30˚C. Precipitation varies greatly, with annual totals ranging from 800 to 2800 mm. The distribution of rainfall throughout the year shows a concentration of over 80% between the months of October to March, with December, January, and February being the wettest months [32]. This rainy period is part of the large-scale phenomenon known as the South Atlantic Convergence Zone, SACZ, one of the most significant phenomena in the summer regional scale in South America. Many flood, inundation, and mass movement events are associated with extreme rainfall caused by SACZ [33].

Due to its steep terrain with valleys, amphitheaters, and rugged scarps, Campos do Jordão experiences a high occurrence of mass movement events and flooding [34] [35] [36]. In January 2000, one of the worst landslides was recorded, resulting in the loss of 10 lives, over 100 injured individuals, and severe damage to 423 houses [37] [38]. The neighborhoods most affected by mass movements in the municipality are Vila Albertina, Santo Antônio, and Britador, located within the Piracuama River basin. Due to the recurrent events, this region of the municipality has been equipped with real-time monitoring devices and sensors, including soil moisture sensors, rain gauges, and river level sensors [39]. The location of these sensors, mapping of landslide risk, drainage, and delineation of the basin are shown in **Figure 2**. The locations of recorded mass movement occurrences from 2009 to 2020 are also depicted.

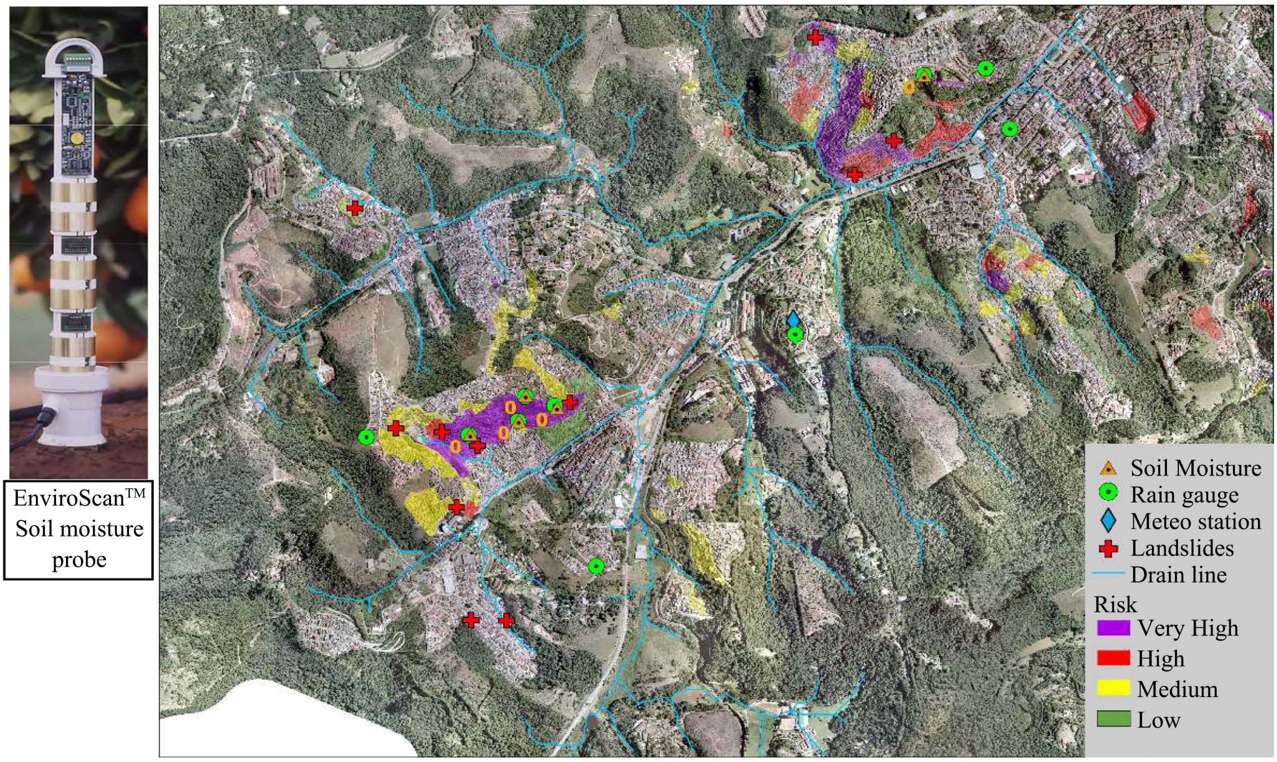

Figure 2. Piracuama River Basin and the location of sensors for monitoring rainfall and soil moisture, river level, as well as landslide risk mapping and records of landslide occurrences.

The moisture sensors shown in **Figure 2** are EnviroScan™ type sensors installed in access tubes manufactured by Sentek Pty. Ltd, containing six capacitive sensors (spaced every 50 cm) distributed along three meters inserted into the soil. The sensors provide outputs in volumetric water content in the soil (millimeters of water per 100 mm of soil). These values are converted from a frequency to a scale using a standard calibration equation, based on data obtained from various scientific studies across a variety of soil textures [37]. The available data from the moisture sensors is limited to the period from 12/04/2019 to the present moment, but the data for December 2019 had to be discarded due to calibration errors. Therefore, the period from 01/01/2020 to 12/31/2021 was defined as the database for analysis in this study.

Figure 3 presents the variations in daily temperature (maximum, minimum, and average daily), the climatological daily average temperature (calculated based on the historical series of the INMET meteorological station, data from 2002 until 2021), daily precipitation, and soil moisture at different depths (50 cm to 300 cm) for one of the sampling points shown in **Figure 2**. A clear distinction between the dry period, starting in April, and the wet period, starting in October, can be observed, with maximum temperatures well above the climatological average. It is also evident that soil moisture at a depth of 50 cm responds to rainfall much more quickly. Regarding temperature, during the dry period, it can be observed that temperatures reach their minimum values, both for daily maximums and minimums.

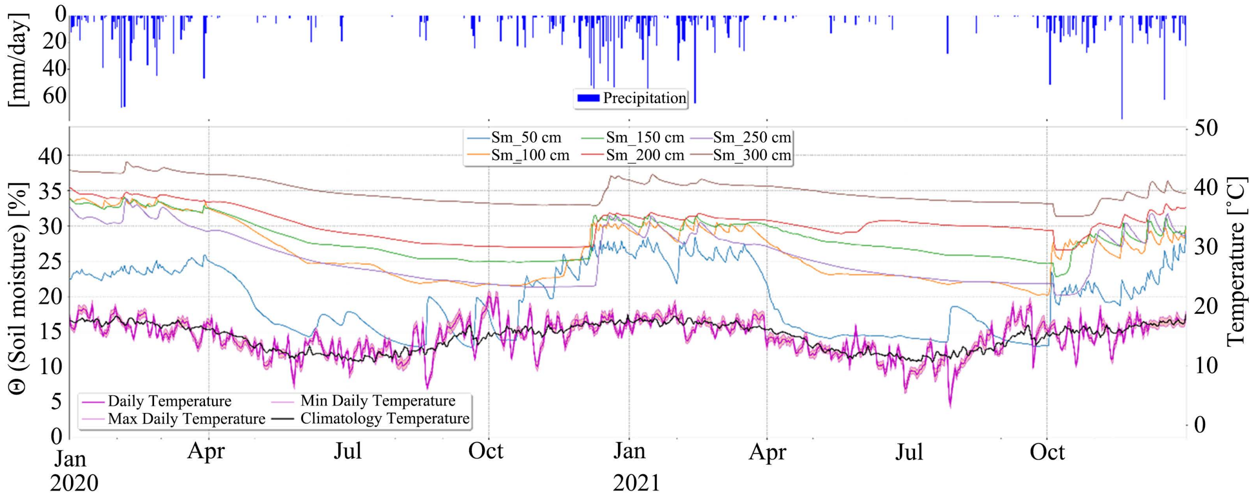

Figure 3. Temperature (maximum, minimum, daily average, and climatological average), precipitation, and recorded soil moisture for different depths (point 1 location in Figure 2).

3. Antecedent Precipitation Index

The Antecedent Precipitation Index (API) is typically used to estimate surface runoff based on recorded rainfall events using rain gauges or other estimation techniques in unmonitored watersheds or those lacking direct calculation information, such as discharge data [40]. Antecedent precipitation is calculated based on the recorded rainfall in the days leading up to the event day it refers to. It can also serve as a measure of soil moisture. The initial condition of the soil in terms of its water content is of crucial importance to have a quantitative understanding, as dry soil responds differently than moist or saturated soil. The physical process can be quite complex, but conceptually, it can be said that the response differs due to the reduction in infiltration capacity [41].

Reference [42] presented an equation for the calculation of API as follows:

$$\mathrm{API} = \sum_{t=-1}^{-i} P_t k^{-t} \,. \tag{1}$$

where i represents the number of antecedent days, k is a decay constant, also known as the recession coefficient, and P_t is the precipitation during day t. This model can also be considered as "retained rainfall" [43].

Equation (1) presents the recession coefficient as constant, which disagrees with the physical processes that vary at different temporal scales. The recession coefficient should consider water losses due to evapotranspiration or drainage. Since evapotranspiration depends on various factors (e.g., temperature, solar radiation, wind speed, among others) that vary throughout the day, the recession coefficient should be calculated to account for this variability. Reference [27] proposed a reformulation in the calculation of the recession coefficient considering only the daily temperature variation, expressed by Equation (2):

$$k = 0.84 + \delta\left(20 - T_{avg}\right). \tag{2}$$

where T_{avg} is the daily average temperature (˚C), and δ is a sensitivity parameter

($^\circ C^{-1}$). The value 0.84 used in the equation is derived from the recommendation of [44], and the temperature of 20˚C is the temperature used when the value 0.84 is considered.

Building upon Equation (2), this work proposes modifications that consider variability in the two constant values used in [27], with the aim of capturing local dynamics, expressed by Equation (3):

$$k = k_{opt} + \delta\left(T_{clt} - T_{avg}\right). \tag{3}$$

where k_{opt} represents the optimized value, for each point where the API is calculated, of the recession coefficient to be determined; T_{clt} is the calculated daily climatological mean temperature based on the recorded historical series. With the modifications, it is expected that the correlation between API and soil moisture will be improved since the parameters will be optimized taking into account the daily temperature variation (difference from the climatological mean) as well as the optimized recession coefficient.

The strategy used to find the optimal values of k_{opt} and δ involved constructing a function, $k\left(t, k_{opt}, \delta, T_{clt}, T_{avg}\right)$, with daily variation ($t$) dependent on the standard recession coefficient (k_{opt}), the sensitivity parameter (δ), and temperatures (T_{clt}, T_{avg}). This function is used to calculate the API (Equation (1)), where the $\mathrm{API}\left(P_t, k, ps, napi\right)$ depends on precipitation (P_t), the recession coefficient (k), calculated for each depth (ps) recorded in the soil moisture sensors (50 cm a 300 cm), and for different numbers of antecedent days ($napi$ = 3, 7, 14, 21, and 28 days).

To achieve the optimal values of the parameters k_{opt} and δ, the resulting API was compared with soil moisture values for different depths, and the Pearson correlation coefficient was calculated. Different combinations of k_{opt} and δ were used to calculate the recession coefficient, aiming to adjust k to better represent the rate of water infiltration into the soil in the studied region. **Figure 4** presents the ranges of values for k_{opt} and δ for different soil depths, considering that 28 days shows the best performance to Pearson correlation showed in **Figure 5**, this number of API days was taken to calculate the API, as well as the region where the correlation coefficients achieve the best results. It can be observed that the depths of 50 cm and 100 cm appear to be the best candidates to establish a relationship between API and soil moisture.

To determine the best correlation coefficients, a search was conducted for all combinations of the parameters k_{opt} and δ (within the intervals according to **Figure 4**), for different soil depths, as well as for different numbers of antecedent API days. **Figure 5** summarizes the search for the best correlation values between soil moisture and API. It can be observed that for API with 3, 7, and 14 days of antecedents (represented by the numbers inside the circles in the figure), in almost all soil depths (except 50 cm), the correlations were below 0.70. For 21 and 28 days, the correlations achieved the best results, with values above 0.7 for depths of 50 cm and 100 cm, and the worst results were for depths of 200 cm and 300 cm. Therefore, to achieve the best correlation, the 28-day API and a depth of

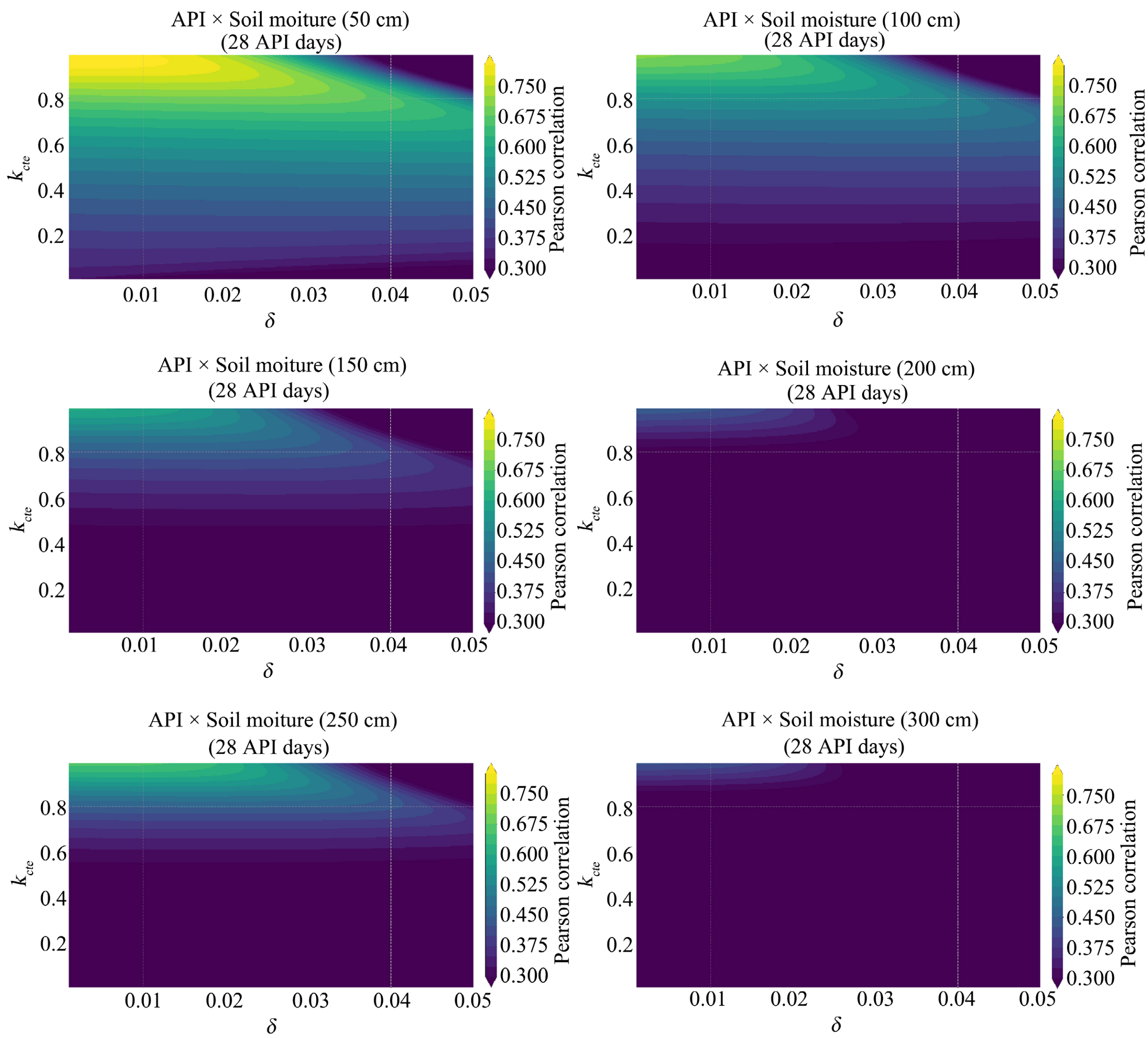

Figure 4. Variation of the parameters k_{opt} and δ, as well as the calculated correlation coefficients for each combination of k_{opt} and δ, represented by the color scale.

50 cm should be used. It should be noted that the correlations were obtained with a limited two-year historical series, which may result in low correlation values and also limit correlations for other depths. Ideally, a good correlation should be achieved with deeper soils, especially at 250 cm depth, as this depth is more characteristic of mass movement events. The 0 cm value in **Figure 5** refers to the average soil moisture calculated based on different depths, which did not show a good correlation.

In [27], the parameter k_{opt} had a fixed value of 0.84, and the value of δ was explored between 0 and 0.03, obtaining the optimal value at 0.012. This optimization was valid for soil moisture up to a depth of 10 cm and API calculated for 3 days in advance, using an 11-year historical series. The limitation on the value of API_{max} was also explored to express the maximum water retention capacity in the

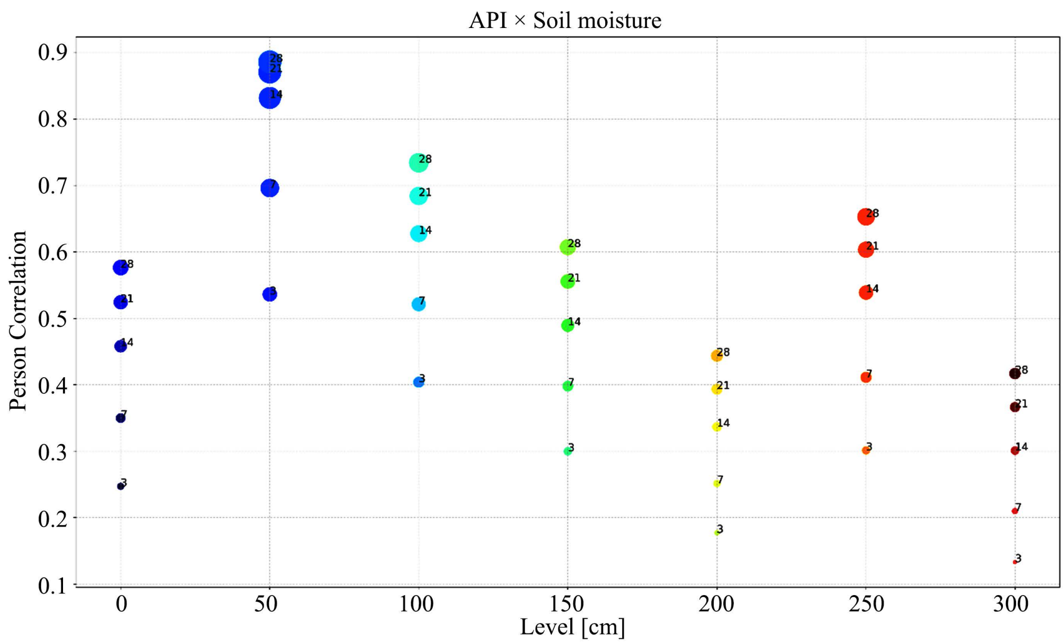

Figure 5. Results of the search for the best Pearson correlation coefficients between soil moisture and API for different soil depths and the number of antecedent days used for API calculation.

soil, which can overestimate soil moisture. This limitation is imposed in the API calculation when it reaches a certain threshold. In [27], the threshold value was set at 35 mm, which considerably improved the correlation between API and soil moisture. This procedure was also used in the proposed API in this work, where the correlation coefficient reached a value of 0.89 at a depth of 50 cm, with $\mathrm{API}_{\max} = 120\ \mathrm{mm}$.

With the optimized parameters, k_{opt} and δ, it was possible to achieve the best API, and from this, adjusted curves were constructed to represent the relationship between API and soil moisture (θ). **Figure 6** presents the scatter plot of $\theta \times \mathrm{API}_c$ (top), with the best-fitted curve exhibiting an exponential behavior and a Pearson coefficient with a value of 0.82. In the lower part, there is the scatter plot of $\theta \times \mathrm{API}_{max}$, with the fitted curve displaying a linear behavior and a Pearson coefficient of 0.89. It can be observed that by limiting the API calculation, the relationship with soil moisture tends to be linear, even using a short two-year historical series.

Since the aim is to establish the API to estimate soil moisture at points where there are no soil moisture sensors and to define thresholds that trigger mass movements, a survey of landslide occurrences in the study area was conducted. The summarized landslide records for the sensor data period (01/01/2020-31/12/2021) are presented in **Table 1**. It is evident that the occurrences were recorded during the rainy period of the municipality, spanning from October to April. **Figure 7** displays the location of the registered landslide events, showing only those that occurred near the soil moisture sensor. This information is crucial for verifying the efficiency of using the API as a soil moisture estimator and consequently establishing thresholds.

Table 1. Landslides recording.

Date	Type	Impact
07/02/2020	On released/natural embankment slope	15 pers./3 homes at risk
09/12/2020	In cut/fill slope launched	3 pers./2 closed houses
09/12/2020	In cut/fill slope launched	16 pers./4 closed houses
09/12/2020	In cut slope	4 pers./1 home at risk
09/12/2020	In cut slope	4 pers./1 home at risk

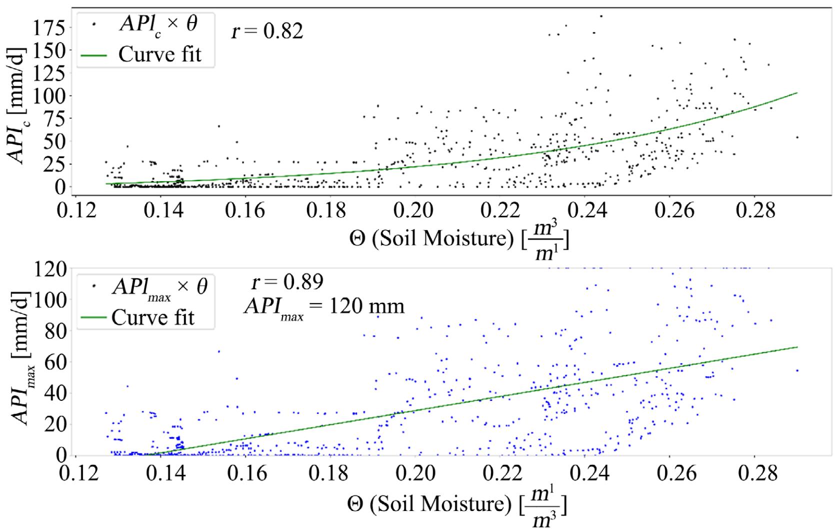

Figure 6. Curve fitting for the API_c and API_{max} indices calculated at a soil depth of 50 cm.

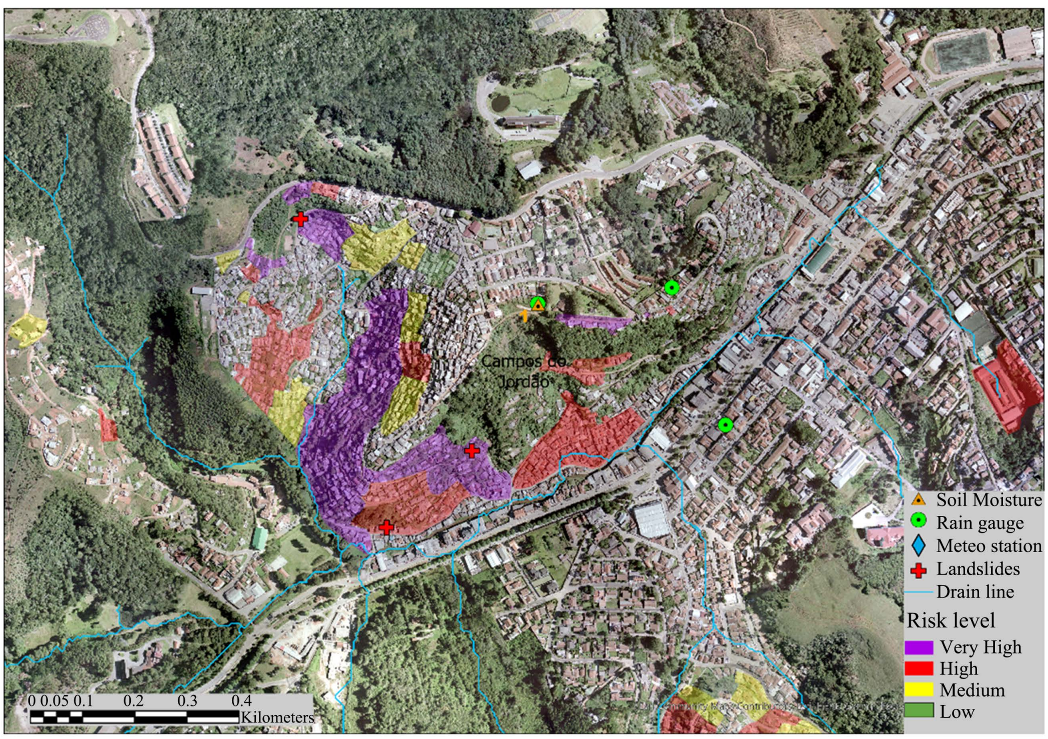

Figure 7. Location of landslide records in 2020.

The performance verification of the API as an index to predict mass movements can be initially observed through Figure 8, where the occurrence of landslides and the values for API_c, API_{max} (Figure 8(a)), observed soil moisture (θ), and soil moisture calculated through API_{max} (Figure 8(b)) are depicted. In Figure 8(a), it can be observed that in the first landslide event (07/02/2020), API_c reached its maximum before the landslide, and in the second event (09/12/2020), the maximum value of API_c coincided. Thus, API_c could not be considered a good predictor since it did not exhibit a consistent behavior during the events. For API_{max}, in both events, the behavior was consistent, where the events occurred above a certain maximum value, indicating good performance in predicting landslide events. Conducting a similar analysis for observed soil moisture and calculated

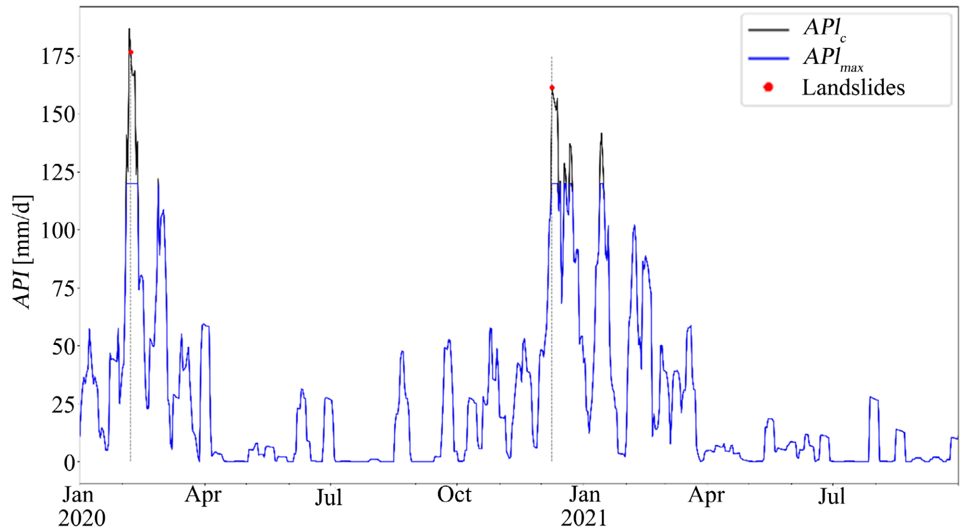

(a)

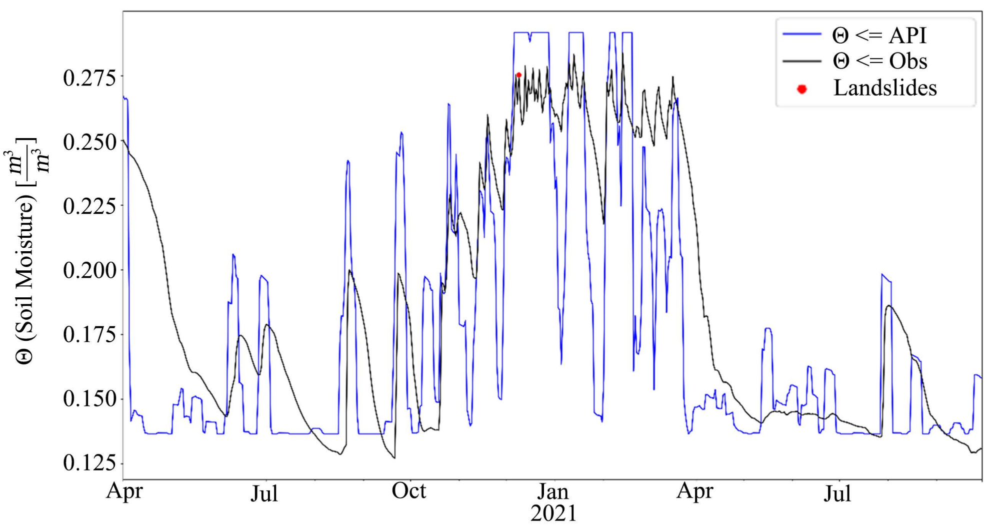

(b)

Figure 8. (a) Variation over the observation period for API_c and API_{max} compared to landslide events. (b) Observed soil moisture and soil moisture calculated through API_{max} (θ_{API}) compared to landslide events.

soil moisture using API_{max}, (θ_{API}) (**Figure 8(b)**), it can be observed that the maximum value was reached before the landslides occurred, also indicating it to be a good predictor of events. It is worth noting that the flattened behavior for the API_{max}, observed in the figures, is due to the cutoff value in accumulated rainfall, as explained previously.

A more detailed analysis of **Figure 8**, highlighting the landslide dates, reveals that θ_{API} reaches a maximum value of 0.29 a few days before the landslides occur on the two distinct dates (**Figure 9**). On the other hand, observed soil moisture shows variations concerning the occurrences, not indicating a clear threshold for landslides. Thus, an initial threshold can be established for the observed point, set at $\theta_{\text{API}} = 0.29$. It is important to note that the historical series, both for soil moisture records and landslide events, is quite short, which could limit the calculated correlations as well as the performance analysis of the API as a potential predictor of mass movements.

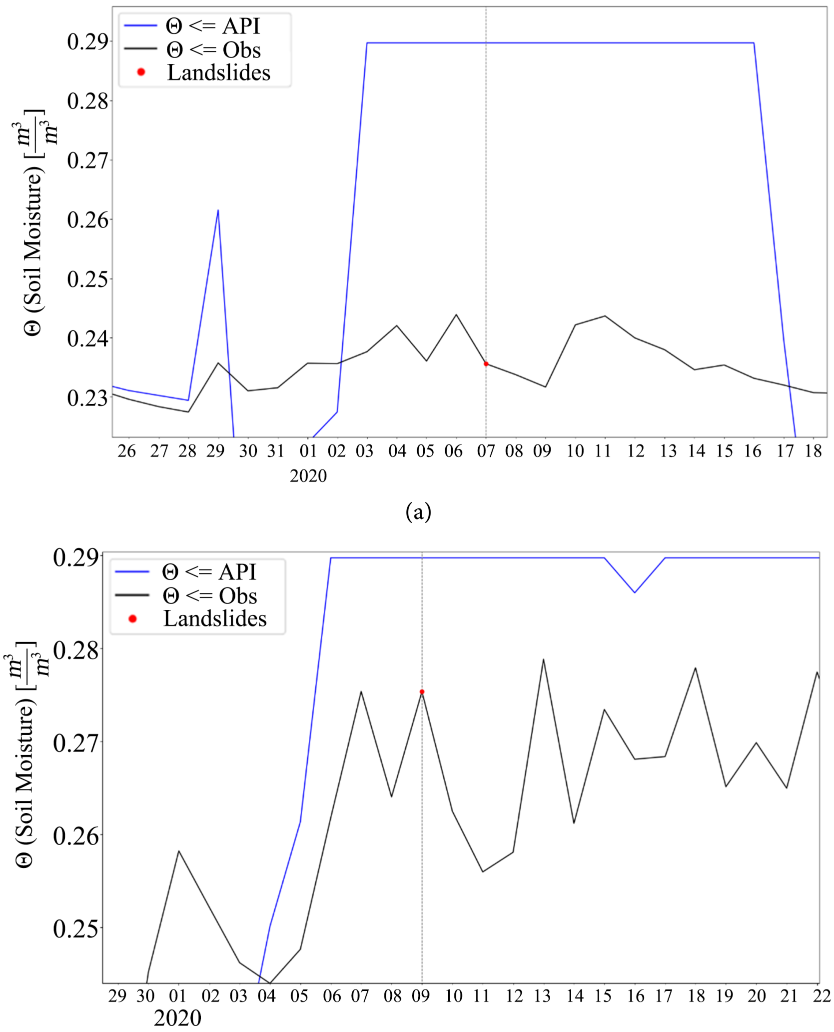

Figure 9. Detail of observed soil moisture variation and θ_{API} for landslide occurrence dates.

4. Conclusion

The objective of this study was to establish a model for calculating the antecedent precipitation index and using it to obtain soil moisture to estimate a critical threshold for mass movements. Despite the short historical series of soil moisture and landslide events, the results have shown promise. Applying the fitted curve to calculate the soil moisture, θ_{API} reached its maximum value ($\theta_{\text{API}} = 0.29$) before the landslides occurred in the verified period, indicating that it can be used as a threshold for the vicinity of the soil moisture sensor (**Figure 7**). The next step of this work will be to expand this model to other regions within the municipality as well as to different historical periods. This expansion will help establish more precise and reliable thresholds. Consequently, this model can be used in a forecasting and mass movement alert system.

Acknowledgements

The authors thank FINEP (Financiadora de Estudos e Projetos) for financing the REDEGEO project (Carta Convite MCTI/FINEP/FNDCT 01/2016), responsible for the PCD Geo network installation and maintenance.

Conflicts of Interest

The authors declare no conflicts of interest regarding the publication of this paper.

References

[1] Aditian, A., Kubota, T. and Shinohara, Y. (2018) Comparison of GIS-Based Landslide Susceptibility Models Using Frequency Ratio, Logistic Regression, and Artificial Neural Network in a Tertiary Region of Ambon, Indonesia. *Geomorphology*, **318**, 101-111. https://doi.org/10.1016/j.geomorph.2018.06.006

[2] Bortolozo, C.A., Andrade, M.R.M., Mendes, T.S.G., Egas, H.M., Moraes, M.A.E., Pryer, T., Prieto, C.C., Metodiev, D., Simões, S.J.C. and Mendes, R.M. (2022) The Tragedy of Morro do Centenário in Petrópolis—RJ, Brazil (February 15, 2022): Landslide Complexity Analyzed from a Multidisciplinary Perspective. https://agu.confex.com/agu/fm22/meetingapp.cgi/Paper/1122883

[3] Coelho-Netto, A.L., de Souza Avelar, A. and Lacerda, W.A. (2009) Landslides and Disasters in Southeastern and Southern Brazil. *Developments in Earth Surface Processes*, **13**, 223-243. https://doi.org/10.1016/S0928-2025(08)10012-8

[4] Bandeira, A.P.N. and Coutinho, R.Q. (2015) Critical Rainfall Parameters: Proposed Landslide Warning System for the Metropolitan Region of Recife, PE, Brazil. *Soils and Rocks*, **38**, 27-48. https://doi.org/10.28927/SR.381027

[5] Pampuch, L.A., Negri, R.G., Loikith, P.C. and Bortolozo, C.A. (2023) A Review on Clustering Methods for Climatology Analysis and Its Application over South America. *International Journal of Geosciences*, **14**, 877-894. https://doi.org/10.4236/ijg.2023.149047

[6] Andrade, M.R.M., Bortolozo, C.A., Carvalho, A.R., Egas, H.M., Garcia, K., Metodiev, D., Nery, T.D., Prieto, C., Pryer, T., Saito, S.M. and Scofield, G. (2023) The SNAKE System: Cemaden's Landslide Early Warning Mechanism. *International Journal of Geosciences*, **14**, 1146-1159. https://doi.org/10.4236/ijg.2023.1411058

[7] Moraes, M.V., Pampuch, L.A., Bortolozo, C.A., Mendes, T.S.G., Andrade, M.R.M. and Metodiev, D. (2023) Thresholds of Instability: Precipitation, Landslides, and Early Warning Systems in Brazil. *International Journal of Geosciences*, **14**, 895-912. https://doi.org/10.4236/ijg.2023.1410048

[8] Metodiev, D., Andrade, M., Mendes, R., Moraes, M., Konig, T., Bortolozo, C.A., Bernardes, T., Luiz, R. and Coelho, J. (2018) Correlation between Rainfall and Mass Movements in North Coast Region of Sao Paulo State, Brazil for 2014-2018. *International Journal of Geosciences*, **9**, 669-679. https://doi.org/10.4236/ijg.2018.912040

[9] Andrade, M., Mascarenhas, M., Metodiev, D., Mendes, T. and Sant'Ana, G. (2023) Análise da chuva e umidade do solo monitorados pela PCD Geotécnica UR12 COHAB II no desastre de maio de 2022 em Recife/PE. Associação Brasileira de Recursos Hídricos, Viamão.

[10] Ashby, B., Bortolozo, C.A., Lukyanov, A. and Pryer, T. (2021) Adaptive Modelling of Variably Saturated Seepage Problems. *Quarterly Journal of Mechanics and Applied Mathematics*, **74**, 55-81. https://doi.org/10.1093/qjmam/hbab001

[11] Sousa, I.A., Bortolozo, C.A., Mendes, T.S.G., Andrade, M.R.M., Dolif, G., Metodiev, D., Pryer, T., Howley, N., Simoes, S.J.C. and Mendes, R.M. (2023) Development of a Soil Moisture Forecasting Method for a Landslide Early Warning System (LEWS): Pilot Cases in Coastal Regions of Brazil. *Journal of South American Earth Sciences*, 131, Article ID: 104631. https://doi.org/10.1016/j.jsames.2023.104631

[12] Bortolozo, C.A., Souza, I.A., Andrade, M.R.M., Mendes, T.S.G., Dolif, G., Pryer, T., Simões, S.J.C., Mendes, R.M. and Metodiev, D. (2022) The Development of a Landslide Alert System Based on the Prediction of Soil Moisture in Critical Cities in Brazil—Preliminary Results with the Cemaden's Observation Network. https://agu.confex.com/agu/fm22/meetingapp.cgi/Paper/1120182

[13] Andrade, M.R.M., Bortolozo, C.A., Mendes, R.M., Metodiev, D., Moraes, M.A.E., Renk, J., Mendes, T.S.G. and Simoes, S.J.C. (2021) Challenges in Implementing a landslide Warning System Based on Soil Moisture Sensors in a Continental-Sized Country Like Brazil—Preliminary Results. *AGU Fall Meeting* 2021, New Orleans, 13-17 December 2021.

[14] Bortolozo, C.A., Mendes, T.S.G., Motta, M.F.B., Simoes, S.J.C., Pryer, T., Metodiev, D., Andrade, M.R.M., Moraes, M.V., Paula, D.S., Bastos, N.J., Pampuch, L.A., Mendes, R.M. and Moraes, M.A.E. (2023) Obtaining 2D Soil Resistance Profiles from the Integration of Electrical Resistivity Data and Standard Penetration Test (SPT) and Light Dynamic Penetrometer (DPL) Resistance Tests. *International Journal of Geosciences*, **14**, 840-854. https://doi.org/10.4236/ijg.2023.149045

[15] Bortolozo, C.A., Mendes, T.S.G., Egas, H.M., Metodiev, D., Moraes, M.V., Andrade, M.R.M., Pryer, T., Ashby, B., Motta, M.F.B., Simoes, S.J.C., Pampuch, L.A., Mendes, R.M. and Moraes, M.A.E. (2023) Enhancing Landslide Predictability: Validating Geophysical Surveys for Soil Moisture Detection in 2D and 3D Scenarios. *Journal of South American Earth Sciences*, **132**, Article ID: 104664. https://doi.org/10.1016/j.jsames.2023.104664

[16] Bortolozo, C.A., Simoes, S.J.C., Andrade, M.R.M., Mendes, R.M., Lavalle, L.V.A., Motta, M.F.B., Metodiev, D. and Mendes, T.S.G. (2019) Guara Registro de Software—Número do Pedido: BR 51 2019 002544-0. *Revista da Propriedade Industrial*, **2549**, 15.

[17] Lavalle, L.V.A., Bortolozo, C.A., Pacheco, T.C.K.F., Andrade, M.R.M., Motta, M.F.B., Mendes, R.M., Metodiev, D., Guedes, M.R.G. and Porsani, J.L. (2018) Evaluation Methodology for Obtaining Geotechnical Parameters Using Electrical Resistivity. *First Break*, **36**, 55-58. https://doi.org/10.3997/1365-2397.n0112

[18] Rangel, R.C., Porsani, J.L., Bortolozo, C.A. and Hamada, L.R. (2018) Electrical Resistivity Tomography and TDEM Applied to Hydrogeological Study in Taubaté Basin, Brazil. *International Journal of Geosciences*, **9**, 119-130. https://doi.org/10.4236/ijg.2018.92008

[19] Hamada, L.R., Porsani, J.L., Bortolozo, C.A. and Rangel, R.C. (2018) TDEM and VES Soundings Applied to a Hydrogeological Study in the Central Region of the Taubaté Basin, Brazil. *First Break*, **36**, 49-54. https://doi.org/10.3997/1365-2397.n0111

[20] Leite, D.N., Bortolozo, C.A., Porsani, J.L., Couto, M.A., Campana, J.D.R., Monteiro Dos Santos, F.A., Rangel, R.C., Hamada, L.R., Sifontes, R.V., Serejo, G. and Stangari, M.C. (2018) Geoelectrical Characterization with 1D VES/TDEM Joint Inversion in Urupês-SP Region, Paraná Basin: Applications to Hydrogeology. *Journal of Applied Geophysics*, **151**, 205-220. https://doi.org/10.1016/j.jappgeo.2018.02.022

[21] Almeida, E.R., Porsani, J.L., Monteiro dos Santos, F.A. and Bortolozo, C.A. (2017) 2D TEM Modeling for a Hydrogeological Study in the Paraná Sedimentary Basin, Brazil. *International Journal of Geosciences*, **8**, 693-710. https://doi.org/10.4236/ijg.2017.85038

[22] Bortolozo, C.A., Couto, M.A., Porsani, J.L., Almeida, E.R. and Monteiro Dos Santos, F.A. (2014) Geoelectrical Characterization Using Joint Inversion of VES/TEM Data: A Case Study in Paraná Sedimentary Basin, São Paulo State, Brazil. *Journal of Applied Geophysics*, **111**, 33-46. https://doi.org/10.1016/j.jappgeo.2014.09.009

[23] Teng W.L., Wang J.R. and Doraiswamy, P.C. (1993) Relationship between Satellite Microwave Radiometric Data, Antecedent Precipitation Index, and Regional Soil Moisture. *International Journal of Remote Sensing*, **14**, 2483-2500. https://doi.org/10.1080/01431169308904287

[24] Zhao, Y., Wei, F., Yang, H. and Jiang, Y. (2011) Discussion on Using Antecedent Precipitation Index to Supplement Relative Soil Moisture Data Series. *Procedia Environmental Sciences*, **10**, 1489-1495. https://doi.org/10.1016/j.proenv.2011.09.237

[25] Ma, T., Li, C., Lu, Z. and Wang, B. (2014) An Effective Antecedent Precipitation Model Derived from the Power-Law Relationship between Landslide Occurrence and Rainfall Level. *Geomorphology*, **216**, 187-192. https://doi.org/10.1016/j.geomorph.2014.03.033

[26] Suribabu, C.R. and Sujatha, E.R. (2019) Evaluation of Moisture Level Using Precipitation Indices as a Landslide Triggering Factor—A Study of Coonoor Hill Station. *Climate*, **7**, Article 111. https://doi.org/10.3390/cli7090111

[27] Zhao, B., Dai, Q., Han, D., Dai, H., Mao, J., Zhuo, L. and Rong, G. (2019) Estimation of Soil Moisture Using Modified Antecedent Precipitation Index with Application in Landslide Predictions. *Landslides*, **16**, 2381-2393. https://doi.org/10.1007/s10346-019-01255-y

[28] Schoener, G. and Stone, M.C. (2020) Monitoring Soil Moisture at the Catchment Scale—A Novel Approach Combining Antecedent Precipitation Index and Radar-Derived Rainfall Data. *Journal of Hydrology*, **589**, Article ID: 125155. https://doi.org/10.1016/j.jhydrol.2020.125155

[29] Ponçano, W.L., Carneiro, C.D.R., Bistrichi, C.A., Almeida, F.F.M. and Prandini, F.L. (1981) Notícia Explicativa do Mapa Geomorfológico do Estado de São Paulo. IPT, São Paulo.

[30] Bistrichi, C.A., Carneiro, C.D.R., Dantas, A.S.L., Ponçano, W.L., Campanha, G.A.C., Nagata, N., Almeida, M.A., Stein, D.P., Melo, M.S. and Cremoni, O.A. (1981) Geo-

logical Map of the São Paulo State IPT/Prominério São Paulo, Scale 1: 5,000,000.

[31] Bortolozo, C.A., Motta, M.F.B., Andrade, M.R.M., Lavalle, L.V.A., Mendes, R.M., Simões, S.J.C., Mendes, T.S.G. and Pampuch, L.A. (2019) Combined Analysis of Electrical and Electromagnetic Methods with Geotechnical Soundings and Soil Characterization as Applied to a Landslide Study in Campos do Jordão City, Brazil. *Journal of Applied Geophysics*, **161**, 1-14. https://doi.org/10.1016/j.jappgeo.2018.11.017

[32] Prince, A.E. (2017) O Clima de Campos do Jordão e a Tuberculose no Século XIX. *ACTA Geográfica*, **11**, 57-74. https://doi.org/10.18227/2177-4307.acta.v11i25.4292

[33] Seluchi, M.E. and Chou, S.C. (2009) Synoptic Patterns Associated with Landslide Events in the Serra do Mar, Brazil. *Theoretical and Applied Climatology*, **98**, 67-77. https://doi.org/10.1007/s00704-008-0101-x

[34] Bortolozo, C.A., Mendes, T.S.G., Motta, M.F.B., Andrade, M.R.M., Lavalle, L.V.A., Mendes, R.M., Simoes, S.J.C., Metodiev, D. and Renk, J. (2021) Geofísica Aplicada em Estudos de Movimentos de Massa e Engenharia de Pequeno Porte. *BOLETIM SBGF*, **116**, 14.

[35] Bortolozo, C.A., Andrade, M.R.M., Mendes, R.M., Mendes, T.S.G., Motta, M.F.B., Lavalle, L.V.A., Simoes, S.J.C., Pampuch, L.A., Pryer, T., Legg, A., Ashby, B., Renk, J. and Metodiev, D. (2021b) How DC and FDEM Methods Can Help Reconstruct the 90-Year History of Occupation of an Urban Area in Campos do Jordão, São Paulo—Brazil and Their Applications in Mass Movement Studies. *AGU Fall Meeting* 2021, New Orleans, 13-17 December 2021.

[36] Bortolozo, C.A., Lavalle, L.V.A., Andrade, M.R.M., Motta, M.F.B., Mendes, R.M., Metodiev, D., Pacheco, T.C.K.F., Guedes, M.R.G. and Porsani, J.L. (2018) Geophysical Methods to Characterize a Mass Movement Event in Tropical Soils in Campos do Jordão City, Brazil. *First Break*, **36**, 71-73. https://doi.org/10.3997/1365-2397.n0115

[37] Mendes, R.M., Andrade, M.R.M., Tomasella, J., de Moraes, M.A.E. and Scofield, G.B. (2018) Understanding Shallow Landslides in Campos do Jordão Municipality—Brazil: Disentangling the Anthropic Effects from Natural Causes in the Disaster of 2000. *Natural Hazards and Earth System Sciences*, **18**, 15-30. https://doi.org/10.5194/nhess-18-15-2018

[38] Mendes, R.M., Valerío Filho, M., Bertoldo, M.A. and da Silva, M.F. (2015) Estudo de limiares críticos de chuva deflagradores de deslizamentos no município de São José dos Campos/SP (Brasil). *Territorium*, **22**, 119-129. https://doi.org/10.14195/1647-7723_22_8

[39] Lavalle, L.V.A., Stabile, R.A., Bortolozo, C.A., Mendes, R.M., Garcia, J.V.C., Motta, M.F.B., Andrade, M.R.M., Pacheco, T.C.K.F. and Metodiev, D. (2018) Environmental Data Observation System—Solam for Analysis and Interpretation of Soil Moisture Variation and Precipitation Indexes. *International Journal of Geosciences*, **9**, 658-667. https://doi.org/10.4236/ijg.2018.911039

[40] Ali, S., Ghosh, N.C. and Singh, R. (2010) Rainfall-Runoff Simulation Using a Normalized Antecedent Precipitation Index. *Hydrological Science Journal*, **55**, 266-274. https://doi.org/10.1080/02626660903546175

[41] Heggen, R.J. (2001) Normalized Antecedent Precipitation Index. *Journal of Hydrologic Engineering*, **6**, 377-381. https://doi.org/10.1061/(ASCE)1084-0699(2001)6:5(377)

[42] Kohler, M.A. and Linsley Jr., R.K. (1951) Predicting Runoff from Storm Rainfall. Weather Bureau, Washington DC.

[43] Singh, V.P. (1989) Hydrologic Systems Watershed Modeling. Prentice-Hall, Englewood Cliffs.

[44] Crozier, M. and Eyles, R. (1980) Assessing the Probability of Rapid Mass Movement. In: *Third Australia-New Zealand Conference on Geomechanics*: *Wellington*, *May* 12-16 1980, Institution of Professional Engineers New Zealand, Wellington, NZ, 2-47-2-51. https://search.informit.org/doi/10.3316/informit.649149381088316